Thermodynamic Temperatures of High-Temperature Fixed Points: Uncertainties Due to Temperature Drop and Emissivity

P. Castro,[1,4] G. Machin,[2] P. Bloembergen,[3] D. Lowe,[2] A. Whittam[2]

[1]University of Cantabria, Santander, 39005, Spain

[2]National Physical Laboratory, Teddington, TW11 0LW, United Kingdom

[3]National Institute of Metrology, NIM, Beijing, 100013, China

[4]To whom correspondence should be addressed. E-mail: castropb@unican.es

Abstract

This study forms part of the European Metrology Research Programme project Implementing the New Kelvin to assign thermodynamic temperatures to a selected set of high-temperature fixed points (HTFPs), Cu, Co-C, Pt-C, and Re-C. A realistic thermal model of these HTFPs, developed in finite volume software ANSYS FLUENT, was constructed to quantify the uncertainty associated with the temperature drop across the back wall of the cell. In addition, the widely applied software package, STEEP3 was used to investigate the influence of cell emissivity. The temperature drop, ΔT, relates to the temperature difference due to the net loss of heat from the aperture of the cavity between the back wall of the cavity, viewed by the thermometer, defining the radiance temperature, and the solid-liquid interface of the alloy, defining the transition temperature of the HTFP. The actual value of ΔT can be used either as a correction (with associated uncertainty) to thermodynamic temperature evaluations of HTFPs, or as an uncertainty contribution to the overall estimated uncertainty. In addition, the effect of a range of furnace temperature profiles on the temperature drop was calculated and found to be negligible for Cu, Co-C, and Pt-C and small only for Re-C. The effective isothermal emissivity ($\varepsilon_{\mathrm{eff}}$) is calculated over the wavelength range from 450 nm to 850 nm for different assumed values of surface emissivity. Even when furnace temperature profiles are taken into account, the estimated emissivities change only slightly from the effective isothermal emissivity of the bare cell. These emissivity calculations are used to estimate the uncertainty in the temperature assignment due to the uncertainty in the emissivity of the blackbody.

Keywords: Emissivity; Eutectics; High-temperature fixed point (HTFP); Temperature drop

1 Introduction

This study forms part of the European Metrology Research Programme project Implementing the New Kelvin [1, 2]. This work inputs into workpackage one (WP1) of that project to assign thermodynamic temperatures to a selected set of high-temperature fixed points (HTFPs) [3], namely, the eutectics Co-C (1597 K), Pt-C (2011 K), and Re-C (2747 K). In addition, the thermodynamic temperature of the Cu point (1358 K) will be measured. The HTFP cells selected for the temperature assignment will be measured by nine different institutes and the temperature values assembled into one consensus temperature as detailed in [4]. When agreeing on a consensus value, it is important to minimize uncertainties, to understand where potential systematic differences between national metrology institutes (NMIs) come from and to identify the differences that are intrinsic to HTFP cells.

Since the definition of the uncertainty budgets for realization of scales by radiation thermometry [5], several papers refining the estimates of the temperature drop and emissivity uncertainties have been published [6, 7, 8]. The aim of this paper is to enable definitive assessment of the uncertainty due to these two effects, as contributors to the HTFP temperature assignment uncertainty.

In this work a realistic thermal model of the actual HTFPs used was constructed to quantify the uncertainty associated with the temperature drop, ΔT, across the back wall of the cavity in the HTFP cell. In addition, specialist software, STEEP3 [9], was used to investigate the effect of the emissivity on thermodynamic temperature determination. The estimated corrections for the emissivity and temperature drop are small compared to other sources of uncertainty in the thermodynamic temperature assignment, and because of that, they are likely to be included in the overall uncertainty assessment as Type B uncertainties rather than corrections [4].

2 Description of the Thermal Model

2.1 Modeling HTFP Cells and Furnace

The HTFP cells were provided by six national measurement institutes as detailed in Table 1, which gives their dimensions as well. The cells of Physikalisch-Technische Bundesanstalt, PTB (Germany); National Metrology Institute of Japan, NMIJ (Japan) and National Institute of Metrology, NIM (China) have the same hybrid design, implying the ingot being surrounded by a graphite sleeve, separated from the crucible by two layers of grafoil. All-Russian Research Institute of Optical and Physical Measurements, VNIIOFI (Russia) provided three different cell designs, Laboratoire National de Métrologie et d'Essais and Conservatoire National des Arts et Metiers, LNE-CNAM (France) used the same (hybrid) design for all their cells and All-Russian Mendeleyev Metrology Institute, VNIIM (Russia) cell had its own design. All the cells were modeled in the same furnace, Type Nagano VR10-A23, one of the furnaces that will typically be used to realize the HTFPs for the assignment of thermodynamic temperature.

The numerical analysis of the melting process was performed by a 2D axisymmetric finite volume model, developed in ANSYS FLUENT [10]. Temperature profiles considered along the furnace tube were (a) uniform temperature profiles at the temperature $T_E + \Delta(T_E)$ where T_E refers to the eutectic temperature and $\Delta(T_E)$ to the offset inducing the melt, which is taken to be from 4 K for Cu up to 20 K for Re-C; and (b) temperature profiles likely to be more extreme than that encountered in actual furnaces were also modeled, the assumption being that the reality will be somewhere between the two extremes modeled.

The thermophysical properties of the materials used in the thermal modeling are detailed in Table 2.

2.2 Temperature Drop Calculations

The temperature drop, ΔT, is related to the temperature difference - due to the net loss of heat from the aperture of the cavity between the back wall of the cavity, viewed by the thermometer defining the radiance temperature, and the solid-liquid interface of the alloy, defining the transition temperature of the HTFP. More specifically, in this work ΔT is defined as this difference at the inflection point of the melting curve, so it includes the temperature drop over the still solid part of the ingot, assuming melting from the outside of the ingot only. It is obvious that ΔT increases with T_E but the modeling performed here shows that its value is always small compared to other contributions to the measurement uncertainty.

The temperature drop, as defined, was calculated for all the cells inside the Nagano furnace with a linear (i.e., uniform) temperature profile along the cell and a sine-shaped temperature profile from the cell aperture to the furnace aperture, as specified in Table 3. It is anticipated that these are extreme cases and that the actual furnace temperature profile likely lies between these two. Earlier work [6] has shown that the actual profile itself does not have a significant influence on the resultant estimated temperature drop values. The temperature profile is maintained in shape but scaled in value for different transition temperatures. As an example, the furnace temperature profile nº 12 is plotted in Fig. 1. The calculated value for this rapid decrease in temperature can be compared with the reference temperature drop for a completely uniform furnace (labeled constant profile in Tables 3 and 4).

With all these different furnace configurations, the melting front of the alloy was modeled and the temperature drop and melting plateaus calculated.

2.3 Effective Emissivity Calculations

The effective emissivity was calculated over the wavelength range from 450 nm to 850 nm by using STEEP3 v1.3 [9] both for the HTFP cells installed in the furnace, and, for reference, for bare HTFP cells (no furnace and with the crucible side wall held at uniform temperature). The surface emissivity for the graphite was assumed to take the conservative range of values of 0.80 to 0.90.

The study reported in [7] showed there would be only small levels of deviation from the ideal blackbody case given reasonable assumptions concerning the furnace temperature profile.

The internal cavity configuration of the cell was the same for NIM, NMIJ, PTB, and LNE, so they presented the same effective emissivity when modeled. The VNIIM and the three VNIIOFI cells differed in cavity length and aperture, so four different models were constructed so as to calculate the effective emissivity of those cells.

The furnace temperature profile used in STEEP3 was derived as an output of the ANSYS FLUENT numerical modeling using the furnace temperature profiles described in Table 3 from the front of the blackbody cavity. The fixed-point blackbody was assumed to be isothermal which is reasonable during a phase transition.

3 Results

3.1 Temperature Drop Estimates

The temperature drop of the cells with the different furnace temperature profiles are given in Table 4a. A consistency check was performed for these results by comparing them with results obtained by previous modeling [8]. The results presented here are obtained from a time-dependent model used to calculate the temperature drop, as defined in Sect. 2.2, at the point of inflection of the melting plateau. These results were found to be very close to the previous ones modeled under steady-state conditions and for similar cells and furnace.

By way of example, Fig. 2 shows the temperature at both sides of the back wall of the cavity during melting with furnace profile nº 13 (uniform temperature profile) for the Re-C NIM cell (11-3). Figure 3 represents the melting plateaus for the same cell (11-3), measured at the back wall of the cavity for the different furnace profiles. Figure 2 shows that the temperature drop is effectively constant over most of the melting curve.

Figure 3 shows that the different furnace profiles do not significantly affect the temperature drop value but do, as expected, influence the melting plateau durations and the position of the points of inflection. It was found that for all the fixed-point cells modeled, the magnitude of the temperature drop was much smaller than other likely sources of uncertainty, for example, at the Re-C point, the best radiometric uncertainty is very likely to be in excess of 0.4 K ($k = 2$), which is five times larger than the estimate of the temperature drop. For the worst case estimate of 0.096 K (Table 4a), this translates to a Type B expanded uncertainty component of $u(\Delta T) = 2 \cdot 0.096/\sqrt{3} = 0.11$ K ($k = 2$), which is much lower than the estimated best radiometric uncertainties.

The uncertainties due to the temperature drop for the fixed points and the different furnace temperature profiles have been calculated, as such, and are presented in Table 4b. The estimated values for the temperature drop are, in relative terms, even smaller as compared to the best radiometric uncertainties for the other HTFPs and, hence, the temperature drop values are likely to be included as Type B estimates in the uncertainty budget for the thermodynamic temperature assignment rather than corrections.

It is clear by examining the values in Table 4a that the estimated values of the temperature drop for Cu, Co-C, and Pt-C were essentially immune to the difference in the furnace temperature profile. In the case of Re-C, there was a small influence observed but this was insignificant compared to the value itself.

From the Re-C temperature drop values some implications can be drawn, referenced in previous studies [6]. The lowest values correspond to the VNIIOFI (nº 17) cell, which has the thinnest back and side walls (1.5 mm) and one of the longest internal cavities (49 mm). Both effects, thinner walls and larger cavities, contribute to decrease the temperature drop on the cavity back wall.

3.2 Effective Emissivity Estimates

The emissivity of the blackbody cavity could be affected by two main variables, the variation in the surface emissivity of the graphite used to manufacture the blackbody cavity and the furnace gradient along and in front of the blackbody cavity. Both these effects were investigated for all the fixed points used in the thermodynamic temperature assignment. Note that in this investigation it was assumed that the cavity itself, during the phase transition, was uniform in temperature because of an intact solid-liquid interface (assuming the melt begins from the outside of the ingot and propagates inwardly) during melting.

3.2.1 Effect of the Isothermal Emissivity of the Fixed Point and the Assumed Uncertainty in the Wall Emissivity

The isothermal emissivity for a range of the blackbody cavities was calculated using STEEP3 for surface emissivity values of 0.8 and 0.9, this being considered the likely range of emissivity values for graphite. Table 5 gives the results of these calculations.

To derive the fixed-point thermodynamic temperature from the radiance temperature, the emissivity of the cavity will have to be corrected for. That correction will be performed as part of the calculation of the single temperature value for each fixed point [4, 11]. For illustrative purposes it is possible to use the isothermal emissivity values in Table 5 to estimate the magnitude of the correction and also its uncertainty.

To estimate the uncertainty of the correction consider the emissivity values for the LNE-NIM-PTB design of the blackbody. This was chosen as the most extreme case as having the widest range of isothermal emissivity values. The uncertainty can be considered as a Type B evaluation based on the difference between the emissivity values i.e., 0.00021. This translates via $\Delta T = (\lambda T_E^2/c_2)\Delta\varepsilon$, to 0.025 K ($k = 1$) uncertainty at the Re-C point for a radiance measurement at 800 nm. An estimate of the temperature correction itself can be derived from the departure from blackbody conditions – in this case the difference from 1 (blackbody) for the average emissivity of the two extremes, 0.999715. This gives a correction of +0.12 K at the Re-C point for an 800 nm radiometer. For all other fixed points the correction for emissivity and its associated uncertainty are less. The conclusion that can be reached is that the correction for emissivity is small compared to other uncertainty sources, but not so small as to be insignificant. For

illustrative purposes Table 6 gives the likely magnitude of the estimated corrections and uncertainties for all the fixed points used for thermodynamic temperature assignment.

3.2.2 Effect of Furnace Gradients in Front of the Blackbody Cavity

Besides the effect of the isothermal emissivity of the actual crucible blackbody cavity described above, there is a possible influence of the furnace on the emissivity of the fixed point. This was investigated through further modeling with STEEP3 including the shape and temperature profile of the furnace in front of the cavity. Two extreme cases were modeled that for a uniform furnace extend from the front of the cavity to a furnace aperture (140 mm away) and that for a furnace with a temperature drop that follows a sine profile decline from the front of the cavity (at the fixed point temperature) to quasi-ambient conditions at the furnace aperture. The aperture diameter of the furnace was 24 mm, and the emissivity of a 1 mm diameter region in the central region of the blackbody back wall was calculated. The assumed surface emissivity for the graphite was 0.85.

It was found that the effect of the furnace on the calculated emissivity values of all the cells was very small – with very little difference from the isothermal case < 0.00002. This is such a small effect that the uncertainty approach described in the section above essentially covers any uncertainty due to the influence of the furnace on the emissivity.

4 Conclusions

The most important conclusion is that there is only a weak dependence of the values of the temperature drop and the effective emissivity with the participant cell design and also with the typical temperature profile expected in the furnace. This means that the anticipated uncertainties associated with the temperature drop across the back wall of the HTFP cell and with the effective emissivity of the cavity are significantly lower than the expected radiometric uncertainties [4]. In the light of these findings, it is recommended that no correction be applied for either of these two effects and, instead, because they are small compared to other uncertainty sources, the numbers presented in this paper enter the uncertainty calculation [11] as a Type B evaluation.

The actual value of the temperature drop scales with the nominal temperature of the HTFP; nevertheless, it is lower than 0.100 K at the Re-C point and lower for the other fixed points.

The analytic expression given in [5] over-estimates the temperature drop effect. As a consequence of this work, more realistic values for the temperature drop have been determined and this will ultimately lead to better estimates of the HTFP temperatures with potential consequences to global temperature metrology.

References

1. G. Machin, J. Engert, R. Gavioso, M. Sadli, E. Woolliams, Int. J. Thermophys., doi: 10.1007/s10765-014-1606-4
2. G. Machin, P. Bloembergen, J. Hartmann, M. Sadli, Y. Yamada, Int. J. Thermophys. **28**, 1976 (2007)
3. G. Machin, in *Proceedings of Ninth International Temperature Symposium*, Los Angeles, *Temperature*: *Its Measurement and Control in Science and Industry*, vol. 8, ed. by C.W. Meyer, AIP Conference Proceedings 1552 (AIP, Melville, NY, 2013), pp. 305-316
4. E.R. Woolliams, P. Bloembergen, G. Machin, in *Proceedings of Ninth International Temperature Symposium*, Los Angeles, *Temperature*: *Its Measurement and Control in Science and Industry*, vol. 8, ed. by C.W. Meyer, AIP Conference Proceedings 1552 (AIP, Melville, NY, 2013), pp. 323-328
5. J. Fischer, M. Battuello, M. Sadli, M. Ballico, S.N. Park, P. Saunders, Y. Zundong, B. Carol Johnson, E. van der Ham, W. Li, F. Sakuma, G. Machin, N. Fox, S. Ugur, M. Matveyev, CCT-WG5 on Radiation Thermometry, "Uncertainty budgets for realisation of scales by radiation thermometry" (Bureau International des Poids et Mesures-BIPM, Sèvres, France, 2003), http://www.bipm.org/cc/CCT/Allowed/22/CCT03–03.pdf. Accessed 10 March 2014
6. P. Castro, G. Machin, M. Villamañan, D. Lowe, Int. J. Thermophys. **32**, 1773 (2011)
7. P. Bloembergen, L. Hanssen, S. Mekhontsev, P. Castro, Y. Yamada, Int. J. Thermophys. **32**, 2623 (2011)
8. P. Castro, P. Bloembergen, Y. Yamada, M. Villamanan, G. Machin, Acta Metrol. Sin. **29**, 253 (2008)
9. A.V. Prokhorov, Metrologia **35**, 465 (1998)
10. www.ansys.com
11. E.R. Woolliams, "Uncertainty Analysis for Filter Radiometry Based on the Uncertainty Associated with Integrated Quantities" submitted to Int. J. Thermophys.

Table 1 List of cells provided from different national measurement institutes and their dimensions. Units in mm

HTFP	NMI and cell name			
Cu	LNE (Cu6)	NMIJ (7ST-1)	PTB (CuVI)	VNIIOFI (Cu2)
Co-C	LNE (6Co2)	NMIJ (7ST-9)	NIM (11-4)	VNIIOFI (C5)
Pt-C	LNE (6Pt1)	NMIJ (7ST-5)	NIM (11-2)	PTB (III)
Re-C	LNE (6Re2)	VNIIM (VM)	NIM (11-3)	VNIIOFI (nº 17)

Cell	Outer diameter	Inner diameter	Cavity diameter	Cavity length	Crucible length	Sidewall thickness
VNIIOFI (Cu2)	24	18	3	35	49	1.5
VNIIOFI (Co5)	24	18	3	33	44.5	1.5
VNIIOFI (nº 17)	24	18	3	35	49	1.5
VNIIM	24	19	3.4	42	50	2.5
NMIJ	24	17	3	33	45	2
NIM	24	17	3	31.5	43	2
LNE-CNAM	24	18.8	3	32	44	2.5
PTB	24	18	3	33	45	2

Table 2 Material properties

Material	Thermal conductivity ($W \cdot m^{-1} \cdot K^{-1}$)	C_p ($J \cdot kg^{-1} \cdot K^{-1}$)	Density ($kg \cdot m^{-3}$)	Melting heat ($J \cdot kg^{-1}$)	T_E (K)
Cu	401	384.6	8020	208667.7	1357.77
Co-C	45	456	7750	272512.85	1597.15
Pt-C	86	204.21	20214	134327.7	2011.05
Re-C	55	214.6	21030	177700	2747.35
Graphite	variable[a]	690	2250		
CC sheets	5	690	700		
Foams	5	370	0.35		
Argon	1.6228	520.65	0.0158		

[a] From 62.78 $W \cdot m^{-1} \cdot K^{-1}$ at 1273.15 K to 36.4 $W \cdot m^{-1} \cdot K^{-1}$ at 2773.15 K

Table 3 Furnace temperature profiles along the cell and from front of the cell to the furnace aperture

Profile number	HTFP	Back side cell	Front side cell	From the front of the cell to the furnace aperture
1	Cu	T_E + 4 K	T_E + 4 K	Constant profile of T_E + 4 K
2	Co-C	T_E + 10 K	T_E + 15 K	Sine profile from T_E + 15 K to 400 K
3	Co-C	T_E + 15 K	T_E + 10 K	Sine profile from T_E + 10 K to 400 K
4	Co-C	T_E + 15 K	T_E + 20 K	Sine profile from T_E + 20 K to 400 K
5	Co-C	T_E + 15 K	T_E + 15 K	Constant profile of T_E + 15 K
6	Pt-C	T_E + 13 K	T_E + 20 K	Sine profile from T_E + 20 K to 400 K
7	Pt-C	T_E + 20 K	T_E + 13 K	Sine profile from T_E + 13 K to 400 K
8	Pt-C	T_E + 20 K	T_E + 27 K	Sine profile from T_E + 27 K to 400 K
9	Pt-C	T_E + 20 K	T_E + 20 K	Constant profile of T_E + 20 K
10	Re-C	T_E + 10 K	T_E + 20 K	Sine profile from T_E + 20 K to 600 K
11	Re-C	T_E + 20 K	T_E + 10 K	Sine profile from T_E + 10 K to 600 K
12	Re-C	T_E + 20 K	T_E + 30 K	Sine profile from T_E + 30 K to 600 K
13	Re-C	T_E + 20 K	T_E + 20 K	Constant profile of T_E + 20 K
14[a]	Re-C	T_E + 30 K	T_E + 20 K	Sine profile from T_E + 20 K to 600 K
15[a]	Re-C	T_E + 30 K	T_E + 40 K	Sine profile from T_E + 40 K to 600 K
16[a]	Re-C	T_E + 20 K	T_E + 20 K	Sine profile from T_E + 20 K to 400 K
17[a]	Re-C	T_E + 20 K	T_E + 20 K	Sine profile from T_E + 20 K to 600 K

[a] Calculated only for NIM (11-3) cell

Table 4

(a) Temperature drop at the back wall of the cavity in the inflection point. Units in kelvin

HTFP	Cell			
Cu	LNE (Cu6)	NMIJ Cu (7ST-1)	PTB (CuVI)	VNIIOFI (Cu2)
Profile[a] nº 1 (constant)	0.003	0.003	0.003	0.003
Co-C	LNE (6Co2)	NMIJ (7ST-9)	NIM (11-4)	VNIIOFI (C5)
Profile nº 2	0.008	0.007	0.007	0.006
Profile nº 3	0.008	0.007	0.007	0.007
Profile nº 4	0.008	0.007	0.007	0.006
Profile nº 5 (constant)	0.008	0.007	0.007	0.005
Pt-C	LNE (6Pt1)	NMIJ (7ST-5)	NIM (11-2)	PTB (III)
Profile nº 6	0.022	0.021	0.021	0.021
Profile nº 7	0.023	0.021	0.021	0.021
Profile nº 8	0.022	0.021	0.021	0.021
Profile nº 9 (constant)	0.020	0.020	0.020	0.020
Re-C	LNE (6Re2)	VNIIM (VM)	NIM (11-3)	VNIIOFI (nº 17)
Profile nº 10	0.094	0.095	0.087	0.081
Profile nº 11	0.096	0.095	0.088	0.083
Profile nº 12	0.093	0.094	0.087	0.078
Profile nº 13 (constant)	0.091	0.094	0.085	0.070
Profile nº 14			0.088	
Profile nº 15			0.086	
Profile nº 16			0.088	
Profile nº 17			0.087	

[a] Furnace temperature profiles described in Table 3

Table 4 continued

(b) Uncertainty due to temperature drop for the fixed points**.** Units in kelvin

HTFP	Cell			
Cu	LNE (Cu6)	NMIJ Cu (7ST-1)	PTB_(CuVI)	VNIIOFI (Cu2)
Profile[a] nº 1 (constant)	0.003	0.003	0.003	0.003
Co-C	LNE (6Co2)	NMIJ (7ST-9)	NIM (11-4)	VNIIOFI (C5)
Profile nº 2	0.009	0.008	0.008	0.007
Profile nº 3	0.009	0.008	0.008	0.008
Profile nº 4	0.009	0.008	0.008	0.007
Profile nº 5 (constant)	0.009	0.008	0.008	0.006
Pt-C	LNE (6Pt1)	NMIJ (7ST-5)	NIM (11-2)	PTB (III)
Profile nº 6	0.025	0.024	0.024	0.024
Profile nº 7	0.027	0.024	0.024	0.024
Profile nº 8	0.025	0.024	0.024	0.024
Profile nº 9 (constant)	0.023	0.023	0.023	0.023
Re-C	LNE (6Re2)	VNIIM (VM)	NIM (11-3)	VNIIOFI (nº 17)
Profile nº 10	0.109	0.110	0.100	0.094
Profile nº 11	0.111	0.110	0.102	0.096
Profile nº 12	0.107	0.109	0.100	0.090
Profile nº 13 (constant)	0.105	0.109	0.098	0.081
Profile nº 14			0.102	
Profile nº 15			0.099	
Profile nº 16			0.102	
Profile nº 17			0.100	

[a] Furnace temperature profiles described in Table 3

Table 5 Range of isothermal emissivity values for the blackbody cavities with different assumed surface emissivity

Institute	Surface emissivity 0.8	Surface emissivity 0.9
LNE-NIM-NMIJ-PTB[a]	0.99961	0.99982
VNIIOFI (nº 17)	0.99971	0.99986
VNIIOFI (Cu2 and C5)	0.99964	0.99982
VNIIM	0.99966	0.99985

[a] LNE, NIM, NMIJ, and PTB use the same cavity design and therefore calculations result in the same effective emissivity

Table 6 Temperature correction and uncertainty due to emissivity for the fixed points**.** Units in kelvin

HTFP	Cell			
Cu	LNE (Cu6)	NMIJ Cu (7ST-1)	PTB_(CuVI)	VNIIOFI (Cu2)
Temperature correction	0.029	0.029	0.029	0.028
Temperature uncertainty (k = 1)	0.006	0.006	0.006	0.005
Co-C	LNE (6Co2)	NMIJ (7ST-9)	NIM (11-4)	VNIIOFI (C5)
Temperature correction	0.040	0.040	0.040	0.038
Temperature uncertainty (k = 1)	0.009	0.009	0.009	0.007
Pt-C	LNE (6Pt1)	NMIJ (7ST-5)	NIM (11-2)	PTB (III)
Temperature correction	0.064	0.064	0.064	0.064
Temperature uncertainty (k = 1)	0.014	0.014	0.014	0.014
Re-C	LNE (6Re2)	VNIIM (VM)	NIM (11-3)	VNIIOFI (nº 17)
Temperature correction	0.120	0.103	0.120	0.090
Temperature uncertainty (k = 1)	0.025	0.023	0.025	0.018

Figure Captions

Fig. 1 Furnace temperature profile Nº 12 along the external wall of the blackbody tube. Origin is set at the backside of the crucible

Fig. 2 Temperature drop between both sides of the back wall of the cavity during melting with furnace profile nº 13 for the Re-C NIM cell (11-3)

Fig. 3 Melting plateaus for the Re-C NIM cell (11-3) with different furnace temperature profiles

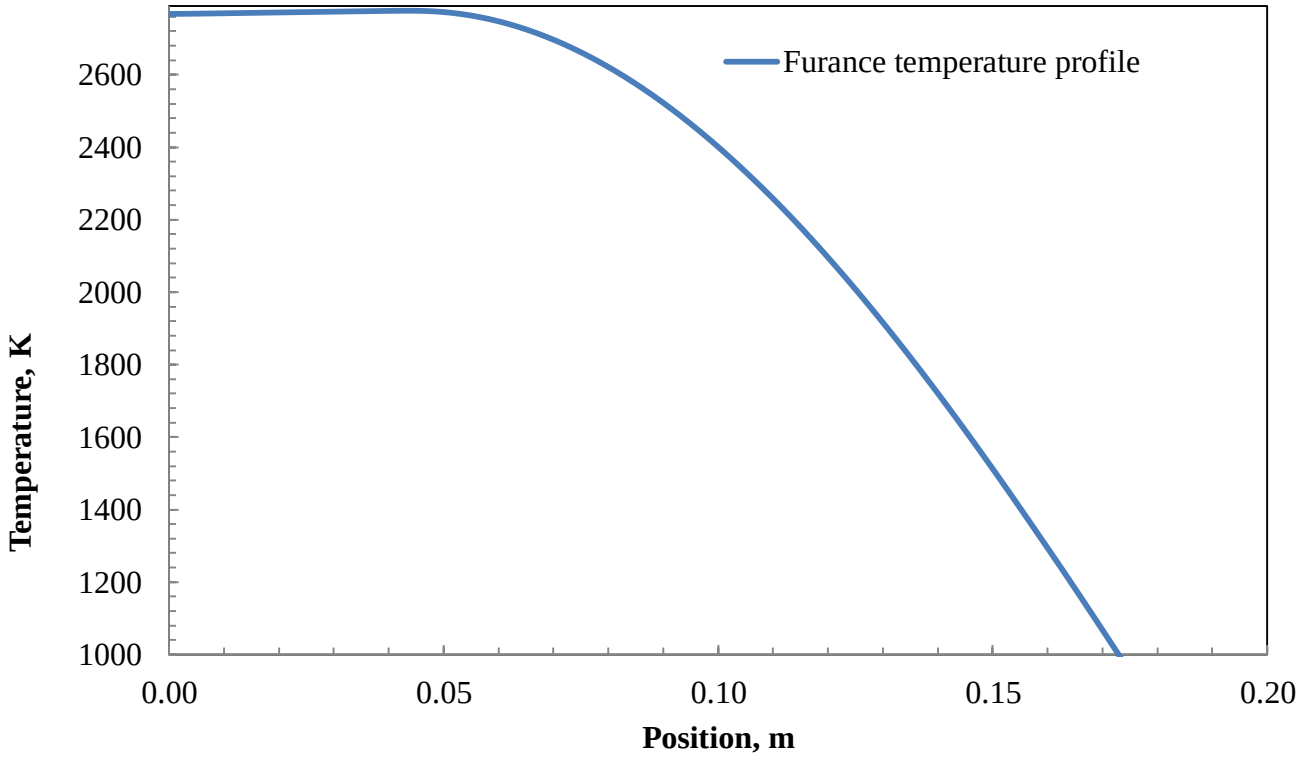
Furance temperature profile
Temperature, K
2600
2400
2200
2000
1800
1600
1400
1200
1000
0.00
0.05
0.10
0.15
0.20
Position, m

Fig. 1

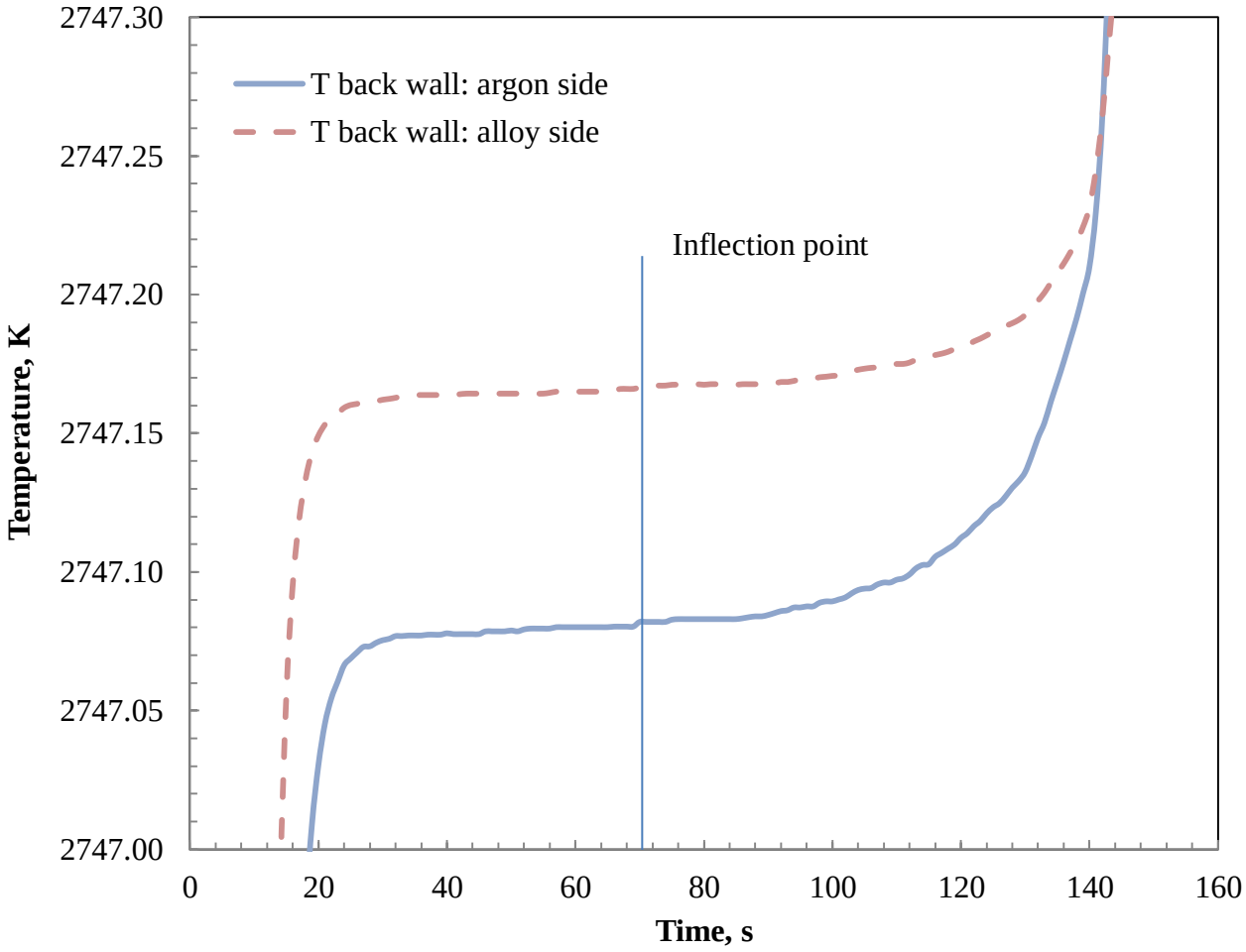
2747.30
2747.25
2747.20
2747.15
2747.10
2747.05
2747.00
Temperature, K
T back wall: argon side
T back wall: alloy side
Inflection point
0
20
40
60
80
100
120
140
160
Time, s

Fig. 2

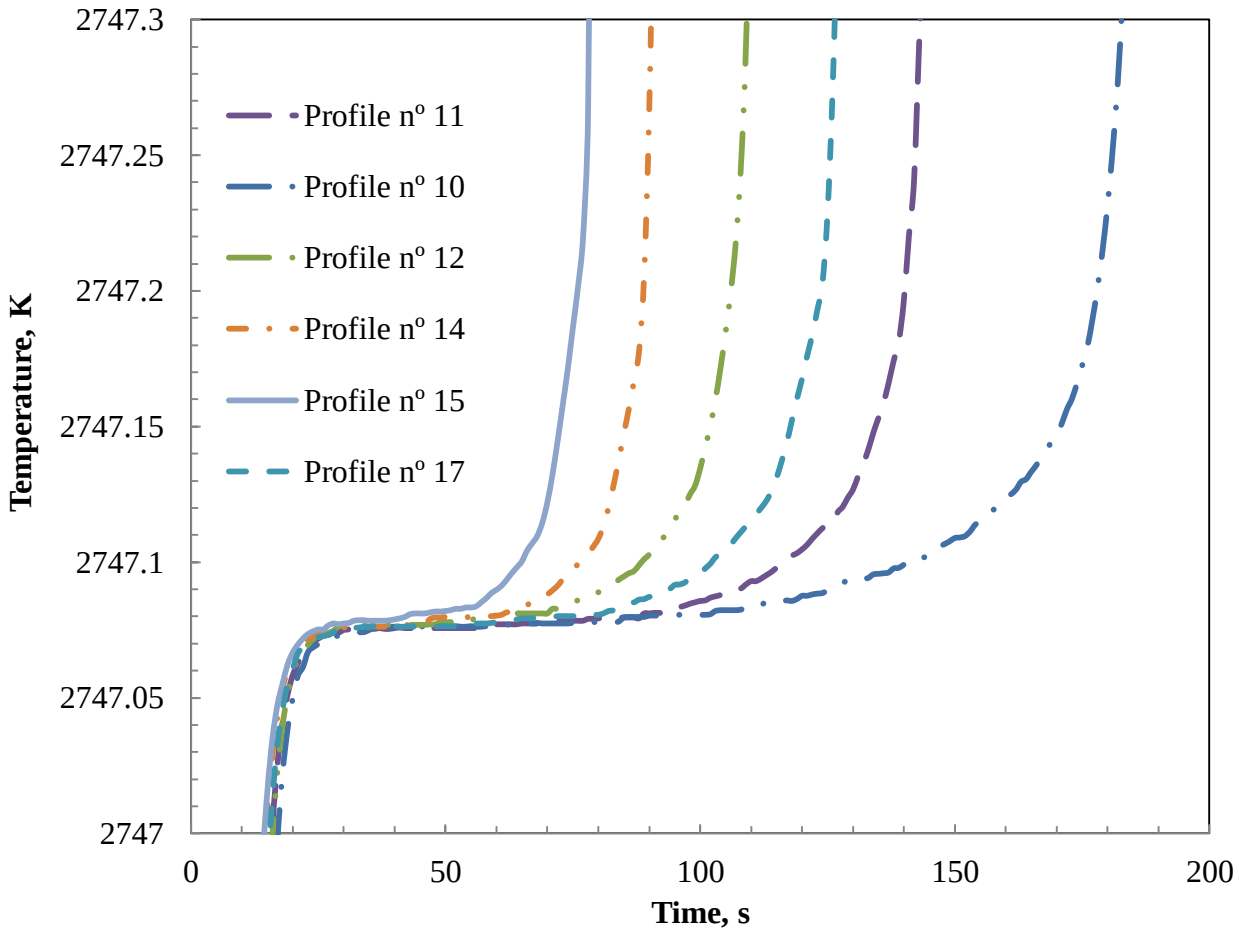
2747.3
2747.25
2747.2
2747.15
2747.1
2747.05
2747
Temperature, K
0
50
100
150
200
Time, s
Profile nº 11
Profile nº 10
Profile nº 12
Profile nº 14
Profile nº 15
Profile nº 17

Fig. 3